Thermal Patterning of a Critical Polymer Blend

A. Voit, A. Krekhov, W. Enge, L. Kramer,† and W. Köhler*

Physikalisches Institut, Universität Bayreuth, D-95440 Bayreuth, Germany

(Received 14 September 2004; published 2 June 2005)

Utilizing the Soret effect, we have employed a moderately focused laser beam (30 μm, 20 mW) to write spatial composition patterns into layers of the critical polymer blend poly(dimethyl siloxane)/poly(ethyl-methyl siloxane) (PDMS/PEMS, $M_w = 16.4/22.8$ kg/mol) both in the one- and in the two-phase region a few degrees above and below the critical temperature $T_c = 37.7\,^{\circ}$C. Because of the critical divergence of the Soret coefficient, moderate temperature gradients are sufficient to induce composition modulations of large amplitude. In the two-phase regime the spinodal demixing pattern can be locally manipulated in a controlled way. 2D simulations based on a modified Cahn-Hilliard equation are able to reproduce the essential spatial and temporal features observed in the experiments.

DOI: 10.1103/PhysRevLett.94.214501 PACS numbers: 47.54.+r, 61.41.+e, 64.60.Fr, 64.75.+g

When a binary fluid mixture enters the two-phase region by crossing its critical point it immediately becomes unstable. Even arbitrarily small composition fluctuations tend to grow and the fluid decomposes into two discrete phases which form an irregular labyrinthine pattern whose characteristic length scale is initially determined by the wave vector with the fastest growth rate. At a later stage of this spinodal decomposition, the pattern coarsens. Close to the critical point, but still in the one-phase regime, the restoring forces vanish, the diffusion dynamics shows a critical slowing down, the amplitude of the fluctuations of the order parameter grows, and the mixture becomes increasingly susceptible to external fields.

The influence of external fields on the demixing process has received growing attention because of the possibility of controlling the demixing morphology. Polymer blends are ideal candidates for such experiments due to their high viscosity, their large correlation length, and the resulting slow dynamics. It has been found that thin films of incompatible polymers, which had been spin coated from a common solvent, resemble the structure of the underlying prepatterned surface [1]. Small filler particles can trigger composition waves in phase-separating polymer blends [2].

The influence of temperature gradients on phase separation has been investigated by a number of authors. Platten and Chavepeyer investigated both the upper (UCST) and lower critical solution temperature (LCST) systems under thermal nonequilibrium conditions in the presence of convection [3]. Yamamura *et al.* [4] observed the formation of stripe patterns in demixing fluids caused by thermocapillary flow and Okinaka *et al.* [5] describe directional phase separation of a polymer blend driven by a temperature gradient. Lee *et al.* [6,7] performed a computational study on the spinodal decomposition process within a temperature gradient. Spatially periodic patterns formed after driving a binary polymer mixture periodically above and below the instability [8]. Kumaki *et al.* [9] observed spinodal decomposition of a ternary polymer solution as much as 20 K above the coexistence temperature after applying a temperature gradient which shifted, due to the Soret effect, the concentration within one region of the sample into the two-phase regime. In all other works involving nonuniform temperature fields, the Soret effect has not been taken into account [4–8].

With the exception of the prepatterned surface, the demixing morphology of the polymer blends is modified in these experiments in a very indirect way by changing some external parameter, like the temperature gradient across the sample. The resultant change in the morphology is recorded, but there is no direct control of the spatial composition pattern. In the following, we will show how composition patterns can directly be written into a critical polymer blend in the vicinity of the critical point, both in the one- and in the two-phase regime, by means of inhomogeneous temperature fields.

A temperature gradient induces a diffusive mass current $\vec{j}_T = -\rho D_T c(1-c)\nabla T$ in a binary mixture due to the Soret effect [10]. ρ is the density of the mixture, c the mass fraction of component one, and D_T the thermal (mass) diffusion coefficient (Soret effect). $\vec{j}_T$ leads to the buildup of a concentration gradient and an accompanying Fickian mass diffusion current $\vec{j}_D = -\rho D \nabla c$. D (> 0 in the one-phase region) is the mutual mass diffusion coefficient. Eventually a stationary concentration gradient

$$\nabla c = -S_T c(1-c)\nabla T \tag{1}$$

is reached where both currents compensate ($\vec{j}_T + \vec{j}_D = 0$). Typical Soret coefficients $S_T = D_T/D$ of ordinary liquid mixtures far away from a phase transition are of the order of 10^{-3} K^{-1} and the resulting concentration difference is only weak [11]. This is, however, no longer true for a mixture in the vicinity of its critical temperature T_c, where S_T shows a critical divergence [12–15].

Recently we have shown for a poly(dimethyl siloxane)/poly(ethyl-methyl siloxane) blend (PDMS/PEMS) that D_T behaves thermally activated with an activation temperature of 1415 K but does not exhibit critical behavior. D shows the well-known critical slowing down on approach of T_c, and S_T diverges like $S_T \propto D^{-1} \propto \epsilon^{-0.67}$ in the critical Ising

regime close to T_c and like $S_T \propto S(0) \propto \epsilon^{-1}$ in the mean field regime further away from the critical point [15]. $S(0)$ is the static structure factor and $\epsilon = (T - T_c)/T_c$ the reduced temperature. Thus, the cause of the divergence of the Soret coefficient is the vanishing of the homogeneity-restoring diffusion current $\vec{j}_D$, whereas $\vec{j}_T$ stays bounded throughout the critical region. Soret coefficients up to $|S_T| \approx 20\ \mathrm{K}^{-1}$ have been found for the PDMS/PEMS blend 0.2 K above T_c. Hence, already moderate temperature gradients should be sufficient to induce noticeable concentration changes. It must, however, be kept in mind that S_T itself is a function of both T and c and falls off rather rapidly away from the critical temperature and the critical composition.

We have tested this idea in a very simple experiment where a focused laser beam (515 nm, 20 mW) has been used for local heating of the sample. The polymer blend PDMS/PEMS with molar masses of $M_w = 16.4$ and 22.8 kg/mol, respectively, was similar to the one which has previously been used for the investigation of transport properties in the critical regime [15]. The blend was at an almost critical composition of $c = 0.536$ (weight fraction of PDMS) with a critical temperature of $T_c = 37.7\,^\circ\mathrm{C}$.

As described in Ref. [15], a minute amount of an inert dye (quinizarin) was added for optical absorption at the laser wavelength. The thickness of the sample was 200 μm and the beam waist approximately 30 μm. The optical density of the sample was 0.1, and we estimate the temperature rise within the beam center to be approximately 5 K. Images of the sample were recorded with a microscope objective (7 ×) and a CCD camera, whose image sensor was, without additional optical elements, within the image plane 50 cm behind the objective. The horizontally oriented sample was illuminated with slightly divergent white light from a cold light source, which produces an observable amplitude image from a pure phase object. This method of imaging of spinodal decomposition patterns in mixtures of nonabsorbing liquids of different refractive indices has been discussed in detail in Ref. [16]. There it has been shown that the visible contrast originates from scattering of light from the phase boundaries. For our sample we estimate the refractive index contrast to approximately 10^{-2} from the Flory-Huggins model. Though the details of the pattern cannot be directly related to the two phases, the spatial periodicity of the domains is correctly reproduced. The equivalency of direct video imaging and structure factor determination by light scattering has been demonstrated both by Guenoun [16] and Harrison [17].

Figure 1 shows the sample at a temperature of approximately 0.8 °C above T_c. The first image [Fig. 1(A)] was taken after 200 sec of exposure at the moment when the laser was switched off. Rather rapidly a sharp rimlike structure develops during exposure which then slowly grows in diameter. Because of the critical slowing down of collective diffusion near the critical point, the cylindrical structure remains, once formed, stable for a long time. Figure 1(B) was taken 100 sec and Fig. 1(C) 15 min after the laser had been switched off. The pattern has lost some of its sharpness and has grown somewhat in diameter, but otherwise it has not lost much of its pronounced features.

The sign of the Soret coefficient is such that PDMS ($n = 1.404$, $T = 20\,^\circ\mathrm{C}$), which has a smaller refractive index than PEMS ($n = 1.428$, $T = 20\,^\circ\mathrm{C}$), migrates to the heated areas, hence towards the optical axis of the laser beam. The thickness of the sample, which is confined between two glass slides, does not change. Further away from T_c the effect becomes weaker and it is not observable with this simple optical setup in ordinary liquids far away from a phase transition. In principle, there is also a thermal lens formed by the heated fluid along the beam path. It is, however, very weak and not visible in the experiment. Because of the short thermal equilibration time, which is of the order of $\tau_{\mathrm{th}} \sim w^2/4D_{\mathrm{th}} \approx 0.5$ ms, the temperature has already equilibrated when the images are recorded. w is the beam waist and D_{th} the thermal diffusivity.

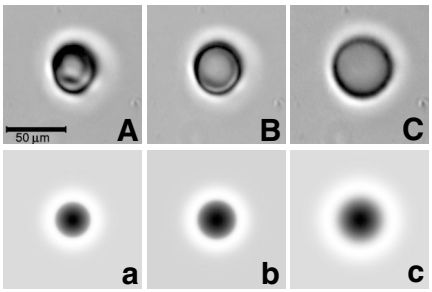

FIG. 1. Temporal development of structure after laser exposure at $T = 38.5\,^\circ\mathrm{C}$, 0.8 °C above T_c. Laser exposure starts at $t = 0$ and ends at $t = 200$ s. Images are taken at $t = 200$ s (A), $t = 300$ s (B), and $t = 1100$ s (C). The lower images (a)–(c) show simulations as described in the text.

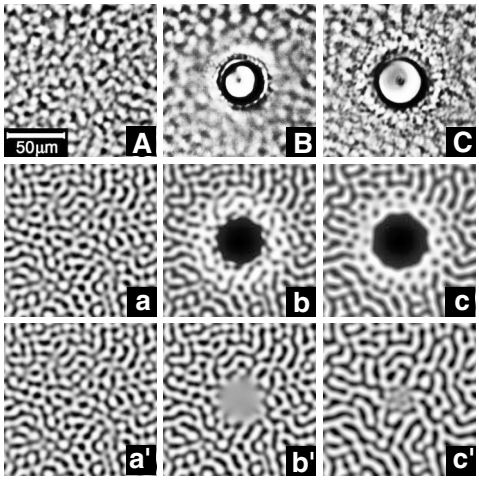

FIG. 2. Temporal development of structure after laser exposure below T_c ($T = 37.2\,^\circ\mathrm{C}$). Laser exposure starts at $t = 0$ and ends at $t = 200$ s. Images are taken at $t = 0$ (A), $t = 300$ s (B), and $t = 700$ s (C). Corresponding images of simulations with (a)–(c) and without (a′)–(c′) Soret effect as described in the text.

Figure 2 shows a similar experiment, except that now the temperature is 0.5 °C below T_c. The sample was quenched into the spinodal regime approximately 120 min prior to switching the laser on. The spinodal decomposition has already reached its intermediate to late stage, characterized by coarsening of the demixing patterns. The Fourier transform of Fig. 2(A) gives a characteristic length scale of the order of 10 μm. Figure 2(A) was taken prior to and Fig. 2(B) 100 sec after an exposure of 200 sec. Since the spatial concentration distribution of the two polymers cannot be extracted quantitatively by direct imaging techniques, the gray scales of the experimental images in Fig. 2 have been equalized for optimum contrast.

The spinodal pattern completely disappears during exposure within the central part of the rimlike structure. After the laser is switched off, this circular pattern again survives for a long time and only slowly deteriorates [Figs. 2(B) and 2(C)]. After turning off the exposure, a concentric ring with a somewhat irregular structure develops, which slowly grows in diameter [Fig. 2(C)] and moves away from the central spot like a spherical wave.

A quantitative description of the stationary solution in the one-phase regime can, in principle, be obtained from Eq. (1) together with the heat equation [Eq. (6) below] for the temperature $T(\vec{r}, t)$ with a suitable source term for the absorbed laser power per unit volume. When compared to holographic measurements of the transport coefficients, which are always performed very close to thermal equilibrium and where the induced concentration perturbations are negligible [15,18], the situation is now more complicated due to the strong temperature and composition dependence of the Soret coefficient. Hence, S_T can no longer be taken as constant in Eq. (1). A quantitative solution of Eq. (1) for a given temperature distribution $T(\vec{r})$ would require the knowledge of S_T as a function of both temperature and concentration. The only data presently available are for the temperature dependence of the Soret and the diffusion coefficient of a critical PDMS/PEMS blend [15], but there are no concentration dependent measurements. We plan to perform such experiments in the future, but a systematic study will require a substantial amount of work and cannot be done within short time.

In order to circumvent this problem, we assume a constant thermal diffusion coefficient, which is justified by the absence of a critical divergence of D_T. To model the effect of phase separation we use the Cahn-Hilliard equation taking into account an inhomogeneous temperature distribution which couples to concentration variation via the Soret effect [19]. We use the Flory-Huggins model for the free energy of mixing of the two polymers. Being a lattice model, the composition is naturally measured in terms of volume fraction ϕ of component A, which is related to the weight fraction c used in Eq. (1) by

$$c = \frac{\phi\rho_A}{\phi\rho_A + (1-\phi)\rho_B}. \tag{2}$$

ρ_A and ρ_B are the densities of the two polymers. Since the densities of PDMS (0.969 g/cm^3) and PEMS (0.977 g/cm^3) are comparable, c and ϕ are almost identical, $\phi \approx c$, and Eq. (1) can as well be written in terms of volume fractions.

For an incompressible binary A/B mixture the continuity equation relates the local volume fraction $\phi(\vec{r}, t)$ to the mass current $\vec{j}(\vec{r}, t)$, and expresses the conservation of mass in the system

$$\rho\frac{\partial\phi(\vec{r}, t)}{\partial t} = -\nabla\cdot\vec{j}(\vec{r}, t), \qquad \vec{j} = \vec{j}_D + \vec{j}_T, \tag{3}$$

where $\vec{j}_D$ and $\vec{j}_T$ have been given above. In the two-phase region the expression for the Fickian diffusion current $\vec{j}_D$ has to be modified. We start from the general expression $\vec{j}_D = -\rho M(\nabla\mu)_T$, where M is the "mobility" of species A with respect to B, and $\mu = \mu_A - \mu_B$ is the difference in chemical potential.

In a Ginzburg-Landau-type continuum description the chemical potential μ is related thermodynamically to the free energy functional $F[\phi(\vec{r}, t)]$ as $\mu = \delta F[\phi]/\delta\phi$. Close to the critical point of spinodal decomposition the free energy of mixing can be approximated by a Taylor expansion with respect to the compositional fluctuation $\varphi(\vec{r}, t) = [\phi(\vec{r}, t) - \phi_c]$ leading to the Ginzburg-Landau (GL) functional

$$\frac{F_{\mathrm{GL}}[\varphi]}{k_BT} = \frac{1}{\upsilon}\int d\vec{r}\left[\frac{1}{2}b\varphi^2 + \frac{1}{4}u\varphi^4 + \frac{1}{2}K(\nabla\varphi)^2\right], \tag{4}$$

where k_B is Boltzmann's constant and υ is the volume per lattice site. Starting from the Flory-Huggins expression for the free energy of mixing one obtains for the coefficients b, u, and K

$$\begin{aligned} b &= 2(\chi_c - \chi) \approx \frac{2\beta}{T_c^2}(T - T_c), \quad u = \frac{4}{3}\chi_c^2\sqrt{N_AN_B}, \\ K &= \frac{1}{18}[\sigma_A^2(1 + \sqrt{N_A/N_B}) + \sigma_B^2(1 + \sqrt{N_B/N_A})]. \end{aligned} \tag{5}$$

Here $\chi = \alpha + \beta T^{-1}$ is the Flory interaction parameter; N_A and N_B are the degrees of polymerization of species A and B, respectively; σ_A and σ_B are the monomer sizes.

The inhomogeneous temperature field produced by light absorption is to be calculated from the heat equation

$$\frac{\partial T(\vec{r}, t)}{\partial t} = D_{\mathrm{th}}\nabla^2T(\vec{r}, t) + \frac{\alpha_\lambda}{\rho c_p}I(\vec{r}, t). \tag{6}$$

The heat source term is proportional to the light intensity I that corresponds to the local illumination of the polymer film. Here α_λ is the optical absorption coefficient and c_p the specific heat at constant pressure. For the polymer blends under experimental study the Lewis number, ratio of the temperature diffusion rate over the mass diffusion rate, is of the order of 10^3. Therefore, one can treat the heat Eq. (6) in the steady limit (neglect the time derivative of the temperature). Equations (3) and (6), in combination with

(4), define our model close to the critical point

$$\frac{\partial \varphi(\vec{r}, t)}{\partial t} = \frac{M k_B T}{v} \nabla^2 [b(T)\varphi + u\varphi^3 - K\nabla^2 \varphi] + D_T \phi_c (1 - \phi_c) \nabla^2 T, \quad (7)$$

$$D_{\text{th}} \nabla^2 T = -\frac{\alpha_\lambda}{\rho c_p} I(\vec{r}, t). \quad (8)$$

Note that the quantity $S_T = D_T/D$ is the Soret coefficient with the diffusion coefficient $D = (M k_B T|b|)/v$. Neglecting the last term Eq. (7) reduces to the well-known Cahn-Hilliard equation (''model B'' [20]).

Numerical simulations of Eqs. (7) and (8) were performed in 2D using a central finite difference approximation of the spatial derivatives with fourth order Runge-Kutta integration of the resulting ordinary differential equations in time. Details of the simulation technique can be found in Ref. [19]. The material parameters of the polymer blend PDMS/PEMS were used, and the spatial scale $\xi = (K/|b|)^{1/2}$ and time scale $\tau = \xi^2/D$ were established from the experimental measurements of the structure factor evolution under a homogeneous temperature quench.

The results of the simulations are shown in Figs. 1(a)–1(c) and in Fig. 2(a)–2(c) for parameters comparable to the experimental conditions. Note that the simulations directly show the A- and B-rich phase as dark and bright areas, whereas the experimental images are generated by an optical imaging technique, from which only characteristic patterns and length scales are directly comparable. We want to point out that the interpretation of the video images generated by pure phase objects is a delicate problem and more work will be necessary towards a fully quantitative description. Nevertheless, the dynamics and characteristic features in the recorded and simulated images can be compared and show good agreement.

Simulations below T_c were also performed without Soret effect [Fig. 2(a′), 2(b′), and 2(c′)] with otherwise identical parameters by setting $D_T = 0$ in Eq. (7). All other parameters of the model were kept constant and the same initial conditions were used [Fig. 2(a) and Fig. 2(a′) are identical). The laser heated spot is brought into the one-phase regime during exposure, but the characteristic features of the experimentally observed demixing pattern do not show up.

Our simulations clearly demonstrate that without thermally driven mass diffusion, the spatial variation of the control parameter $b(T)$ due to the local laser heating does not provide the typical pattern evolution observed in the experiments. In contrast, taking into account the Soret effect, a behavior quite similar to the one experimentally observed was found, although the simulations were done in 2D.

We have demonstrated that long-living spatial composition patterns with lifetimes of many hours can be written into a polymer blend in the vicinity of its critical point by local laser heating. Since the Soret coefficient exhibits a critical divergence at T_c, moderate temperature gradients are sufficient. In the two-phase regime, the spinodal demixing pattern can locally be manipulated on a mesoscopic length scale. We expect the smallest achievable structures to be in the region of the diffraction limit of the laser beam. Using simulations based on an extension of the Cahn-Hilliard model, we have been able to reproduce the essential features observed in the experiment. This new effect is not limited to the cylindrical geometries discussed in the present work and may possibly open a new route towards the structuring of polymer blends and towards the creation of gradient materials and embedded gradient structures.

We thank G. Meier for the samples and for helpful discussions. This work was supported by the *Deutsche Forschungsgemeinschaft* (SFB481/A8).

*Electronic address: werner.koehler@uni-bayreuth.de
†Deceased.

[1] M. Böltau *et al.*, Nature (London) **391**, 877 (1998).
[2] B. P. Lee, J. F. Douglas, and S. C. Glotzer, Phys. Rev. E **60**, 5812 (1999).
[3] J. K. Platten and G. Chavepeyer, Physica A (Amsterdam) **213**, 110 (1995).
[4] M. Yamamura *et al.*, Polymer **44**, 4699 (2003).
[5] J. Okinaka and Q. Tran-Cong, Physica D (Amsterdam) **84**, 23 (1995).
[6] K.-W. D. Lee, P. K. Chan, and X. Feng, Macromol. Theory Simul. **11**, 996 (2002).
[7] K.-W. D. Lee, P. K. Chan, and X. Feng, Macromol. Theory Simul. **12**, 413 (2003).
[8] H. Tanaka and T. Sigehuzi, Phys. Rev. Lett. **75**, 874 (1995).
[9] J. Kumaki, T. Hashimoto, and S. Granick, Phys. Rev. Lett. **77**, 1990 (1996).
[10] S. R. de Groot and P. Mazur, *Non-Equilibrium Thermodynamics* (Dover, New York, 1984).
[11] J. K. Platten *et al.*, Philos. Mag. **83**, 1965 (2003).
[12] D. W. Pohl, Phys. Lett. **77A**, 53 (1980).
[13] M. Giglio and A. Vendramini, Phys. Rev. Lett. **34**, 561 (1975).
[14] W. Enge and W. Köhler, Chem. Phys. Chem. **5**, 393 (2004).
[15] W. Enge and W. Köhler, Phys. Chem. Chem. Phys. **6**, 2373 (2004).
[16] P. Guenoun, R. Gastaud, F. Perrot, and D. Beysens, Phys. Rev. A **36**, 4876 (1987).
[17] C. Harrison, W. Rippard, and A. Cumming, Phys. Rev. E **52**, 723 (1995).
[18] G. Wittko and W. Köhler, Philos. Mag. **83**, 1973 (2003).
[19] A. P. Krekhov and L. Kramer, Phys. Rev. E **70**, 061801 (2004).
[20] P. C. Hohenberg and B. I. Halperin, Rev. Mod. Phys. **49**, 435 (1977).